



Effect of material thermo-viscoplastic modeling on the prediction of forming limit curves of aluminium alloy 5086

Xingrong Chu, Lionel Leotoing, Dominique Guines, Eric Ragneau

► To cite this version:

Xingrong Chu, Lionel Leotoing, Dominique Guines, Eric Ragneau. Effect of material thermo-viscoplastic modeling on the prediction of forming limit curves of aluminium alloy 5086. *Journal of Materials Engineering and Performance*, 2015, 24 (9), pp.3459-3470. 10.1007/s11665-015-1643-6 . hal-01186216

HAL Id: hal-01186216

<https://hal.science/hal-01186216>

Submitted on 24 Aug 2015

HAL is a multi-disciplinary open access archive for the deposit and dissemination of scientific research documents, whether they are published or not. The documents may come from teaching and research institutions in France or abroad, or from public or private research centers.

L'archive ouverte pluridisciplinaire **HAL**, est destinée au dépôt et à la diffusion de documents scientifiques de niveau recherche, publiés ou non, émanant des établissements d'enseignement et de recherche français ou étrangers, des laboratoires publics ou privés.

Effect of material thermo-viscoplastic modeling on the prediction of forming limit curves of aluminium alloy 5086

Xingrong Chu^{1*}, Lionel Leotoing², Dominique Guines², Eric Ragneau²

¹ School of Mechanical, Electrical and Information Engineering, Shandong University, Weihai, 264209, China

² Université Européenne de Bretagne, INSA-LGCGM, CS 70839, 20 avenue des Buttes de Coësmes, 35708 Rennes Cedex 7, France

Abstract: A solution to improve the formability of aluminium alloy sheets can consist in investigating warm forming processes. The optimization of forming process parameters needs a precise evaluation of material properties and sheet metal formability for actual operating environment. Based on the analytical M-K theory, a Finite Element (FE) M-K model was proposed to predict Forming Limit Curves (FLCs) at different temperatures and strain rates. The influences of initial imperfection value (f_0) and material thermos-viscoplastic model on the FLCs are discussed in this work. The flow stresses of AA5086 were characterized by uniaxial tensile tests at different temperatures (20, 150 and 200°C) and equivalent strain rates (0.0125, 0.125 and 1.25 s⁻¹). Three types of hardening models (power law model, saturation model and mixed model) were proposed and adapted to correlate the experimental flow stresses. The three hardening models were implemented into the FE M-K model in order to predict FLCs for different forming conditions. The predicted limit strains are very sensitive to the thermo-viscoplastic modeling of AA5086 and to the calibration of the initial geometrical imperfection which controls the onset of necking.

Keywords: Sheet forming; Forming Limit Curves (FLCs); FE M-K model; Thermo-viscoplastic modeling; Aluminium alloys

1. Introduction

Due to their high specific strength and stiffness, lightweight materials such as aluminium alloys have received a full attention to improve fuel economy in transportation industry. However, the poor formability of these materials at ambient temperature greatly limits their applications, especially for the manufacturing of components with complex shapes. Thanks to innovative warm forming techniques, the formability can be improved at elevated temperatures. During sheet metal forming process, the formability may depend on many factors like material properties and process conditions (strain path, strain rate, temperature,...). From literature, aluminium alloys become generally strain-rate dependent materials when temperature increases from ambient conditions to high values, above 150°C. Hence, characterizing the sheet metal formability at elevated temperatures and for a wide range of strain rates is essential for an efficient optimization of the forming process parameters.

The prevalent technique to evaluate the sheet metal formability is the forming limit diagram (FLD). In the FLD, the forming limit curve (FLC) is a combination of minor and major strains corresponding to the onset of through-thickness necking localizations for different linear strain paths. The determination of FLCs has always been a worrying topic in the last decades with the development of experimental, analytical or numerical approaches. Two kinds of standard formability tests are proposed in the international standard: Nakazima (out-of-plane) stretching and Marciniak (in-plane) stretching tests. By forming specimens with different widths, the whole FLC with the limit strains covering the strain paths from uniaxial tension through plane strain tension to equibiaxial tension can be obtained.

In the literature, very few experimental works about the formability of aluminium alloy sheets combining both temperature and strain rate effects can be found. Naka et al. [1] established the FLCs of AA5083-O under different forming speeds (0.2 to 200 mm/min) and forming temperatures (20 to 300°C) with a Marciniak test setup. It was proved that the formability increased with the increasing temperatures and decreasing forming speeds. The formability (in terms of elongation) of AA5754, AA5182 and AA6111-T4 was studied by Li and Gosh [2] under different temperatures (200 to 350°C) and strain rates (0.015 to 1.5s⁻¹). The total elongation in uniaxial tension was found to increase with temperature and decrease with increasing strain rate. In another work of Li and Ghosh [3], the formability of the above three aluminium alloys was studied from 200 to 350°C, at a strain rate of 1s⁻¹. A positive temperature effect on the sheet formability was observed, but the intensity of the improvement depended on the alloy series. The Limit Drawing Ratio (LDR) of AA5754-O was investigated by Palumbo and Tricarico [4]. By comparing with ambient temperature, a noteworthy increase of LDR (44%) was obtained at a punch speed of 1 mm/min and at a temperature of 110°C in the blank center. The deep drawing and stretch formability of AA7075 was investigated by Hui et al. [5] through the limiting drawing ratio test and the limit dome height test. It was found that the sheet formability could be significantly improved when the blank was heated to 140 - 220 °C while it began to decrease with temperatures over than 260 °C.

The experimental evaluation of formability is a very time consuming procedure. Many predictive models of FLCs work at ambient temperature but very few studies concern the temperature and strain rate effects. A very extensive work was done by Abedrabbo et al. to develop a temperature-dependent anisotropic material model associated with a temperature and strain rate-dependent hardening model, for use in a coupled thermo-mechanical finite element analysis.

The model was developed for aluminium alloys AA3003-H111 [8], AA5182-O and AA5754-O [10]. With a user material subroutine, temperature-dependent Barlat YLD96 and Barlat YLD2000-2d yield functions were used to carry out a finite element analysis of stamping with hemispherical punch. Failure criteria used in the analysis were based on FLCs. The M-K model was used to calculate the different FLCs ([9], [10]) but only temperature was considered. Strain rate effect on FLCs was not evaluated. It was shown that two hardening models (power law and Voce) can give very different FLCs for the same imperfection value. The choice of the imperfection value was not discussed since the predictive FLCs were not compared with experimental ones. A constitutive model was chosen by Khan and Baig [7] to predict FLCs for AA5182 with temperature and strain rate effects but the study remains on the theoretical aspect, and without experimental validation and details concerning the calibration of the M-K model with the imperfection value. Recently, Chu et al. [6] have investigated experimentally the AA5086 formability at different temperatures (20 to 200°C) and strain rates (from 0.02 to 2s^{-1}) to discuss the validity of the well-known predictive M-K model. It was shown that a calibration step is essential to give a reliable prediction of this model. Indeed, the results are strongly dependent on the initial imperfection value which is defined to cause the onset of necking. Moreover, the model must include the thermo-viscoplastic behaviour of the material in order to give the reliable predictive FLCs.

Over recent years, several thermo-viscoplastic constitutive models have been developed for computational mechanics. These models have been classified into two major groups: physical based models and phenomenological based models. For physical based models (Zerilli and Armstrong [11], Bergström [12], Nemat-Nasser and Li [13], Voyiadjis and Abed [14] or Rusinek and Klepaczko [15]), although they are derived from microstructure observation (e.g. dislocation

evolution theory), the material parameters are usually identified from macroscopic material tests. Considering the high number of material constants to be determined, their applications are limited. For the thermo-viscoplastic behavior of aluminium alloys, a modified physical based Bergström model was proposed by van den Boogaard and Bolt [16] to describe the flow stresses of AA5754-O under different temperatures (100, 175 and 250°C) and strain rates (0.002, 0.02s⁻¹). The predictions agreed well with experimental data obtained from monotonic tensile tests. Vegter et al. [17] have presented an extended Bergström model to study the prediction of strain distribution on AA5182 stretch forming parts. This extended model was also adopted by Palumbo and Tricarico [4] to study the formability of AA5754-O. Good correlation between numerical and experimental punch loads was obtained. An extended R-K model was used by Rusinek and Rodríguez-Martínez [18] to describe the negative strain rate behavior of AA5083-H116 at different strain rates (from 0.0004 to 1300s⁻¹) at ambient temperature.

The phenomenological models provide a definition of the material flow stress based on experimental observations. Compared to physical based models, they usually present simple expressions with a reduced number of material constants. Their implementation into Finite Element (FE) codes is generally easy. Although their validity can be limited to a range of temperatures and strain rates due to their empirical nature, these models are widely used. They are usually based on a multiplicative formulation which includes strain, strain rate and temperature functions. Power law type models and saturation type (Voce's type) models are frequently used for aluminium alloys. Abedrabbo et al. [9] have proposed a modified power law model to study the flow stresses of AA3003-H111 in a thermo-forming analysis at different temperatures (25 to 260°C) and strain rates (0.001 to 0.08s⁻¹). The coefficients of the power law model were fitted as functions of temperature

and this model gave accurate punch load curves. By fitting uniaxial tensile test results, different formulations of Voce's models were used to describe the flow stresses of three aluminium alloys (AA6016-T4, AA5182-O and AA5182) by Aretz [19]. Good correlations were obtained compared to experimental results. The true stress-strain response of AA5182-O was modeled by Khan and Baig [7] with a modified KHL model over a wide range of strain rates (10^{-4} to 1s^{-1}) and temperatures (23 to 200°C). In all these studies, hardening laws are typically identified from simple tensile tests due to the difficulties in carrying out advanced tests at high strains (bulge tests, ...) for these conditions of temperature and strain rate. Limit homogeneous equivalent strain observed in tensile tests is generally below 20%, so a significant uncertainty remains on the identified law ability to describe behavior of the material for high strain levels and especially for forming limit predictions (up to 50%).

In this work, to study the effect of the identified material hardening model uncertainty on the prediction of FLCs for an aluminium alloy 5086-H111, three very different constitutive models (a power law, a saturation and a mixed model) are chosen. Based on the flow stresses obtained from uniaxial tensile tests for a defined range of temperature and strain rate, the fitting parameters of the three models are identified. The hardening models are then implemented into a Finite Element model of the geometrical M-K model to determine FLCs for the same range of temperatures and strain rates. The numerical results are then compared to experimental FLCs obtained for the same conditions. Finally, the role of the hardening models coupled with the procedure of calibration of geometrical imperfection values of the M-K model is discussed.

2 Identification of the AA5086 thermo-viscoplastic behaviour

2.1 Hardening models

In order to describe the thermo-viscoplastic behaviour of AA5086, three very different types of hardening models are selected: a power law (Ludwick's type) model, a saturation (Voce's type) model and a mixed type (H-V) model. The H-V model, proposed by Sung et al. [20], incorporates a linear function $\alpha(T)$ which gives power law a high weight for low temperatures and a predominant role of saturation behaviour at elevated temperatures. Based on the experimental stress-strain curves and by considering the evolution of the related parameters with forming temperatures and speeds, the final proposed hardening models are shown in Eq. 1 to Eq. 3.

Ludwick's model:

$$\bar{\sigma} = \sigma_0(T) + (K_0 - K_1 T) \bar{\epsilon}_p^{(n_0 - n_1 T)} \dot{\bar{\epsilon}}_p^{m_0 \exp(m_1 T)} \quad (1)$$

Voce's model:

$$\bar{\sigma} = \sigma_0(T) + K_3 \exp(-K_4 T) \sqrt{1 - \exp(-K_5 \exp(K_6 T) \bar{\epsilon}_p)} \dot{\bar{\epsilon}}_p^{m_2 \exp(m_3 T)} \quad (2)$$

H-V model:

$$\begin{cases} \bar{\sigma} = \sigma_0(T) + (\alpha(T) f_H + (1 - \alpha(T)) f_V) \bar{\epsilon}_p^{m_4 \exp(m_5 T)} \\ \alpha(T) = \alpha_1 - \alpha_2 (T - T_0) \\ f_H = K_7 \bar{\epsilon}_p^{n_2} \\ f_V = K_8 (1 - \exp(-K_9 \bar{\epsilon}_p)) \end{cases} \quad (3)$$

Where $\bar{\epsilon}_p$ and $\dot{\bar{\epsilon}}_p$ are respectively the equivalent plastic strain and the equivalent plastic strain rate. K_i ($i = 0..9$), n_i ($i = 0..2$) and m_i ($i = 0..5$) are material constants.

$\sigma_0(T)$ is the initial yield stress varying with temperatures. Its expression is given by:

$$\sigma_0(T) = \sigma_0 \left(1 - \frac{T}{T_m} \exp \left(Q \left(1 - \frac{T_m}{T} \right) \right) \right) \quad (4)$$

Where $\sigma_0 = 134.6 \text{ MPa}$ is the initial yield stress at ambient temperature, $T_m = 627^\circ \text{C}$ is the

melting temperature and $Q=0.556$.

2.2 Identification results

To identify the AA5086 hardening behaviour, uniaxial tensile tests were carried out at different temperatures (20, 150 and 200°C) and tensile speeds (1, 10 and 100 mm/s). The details of the uniaxial tensile tests were introduced in [6]. The tested specimen has a gage length of 80mm, a width of 10mm and a thickness of 2mm. The tests were carried on a servo-hydraulic testing machine equipped with a dedicated heating device. Experimental results are shown in Figure 1 to Figure 3. For AA5086, depending on the forming conditions (for low temperatures and strain rates), Portevin-Le Chatelier (PLC) bands were observed which manifest as serrations in the hardening curves. To facilitate the reading of Figure 1 to Figure 3, experimental curves have been smoothed but the parameter identification has been performed with raw data, without smoothing. With the selected specimen, the three tensile speeds permit to reach a range of equivalent strain rates from 0.0125 to 1.25s⁻¹. By comparing the experimental flow stresses (Figure 1 to Figure 3), it is noticeable that the mechanical response of AA5086 is not only dependent on temperature but also on strain rate level. As an example, for a strain level close to 20% and for a temperature of 200°C, the flow stress increases from 245MPa at 1mm/s (Figure 1) to 280MPa at 100 mm/s (Figure 3). For these conditions, the increase of flow stress with strain rate is close to 15%. The temperature has a softening effect on flow stress of AA5086. Flow stress decreases with the increase of temperature and the softening effect is emphasized for low forming speeds. The increase of flow stress with forming speed is weak at ambient temperature (for a strain level close to 20%, flow stress value is stable and is about 320MPa at 1mm/s (Figure 1) and 100 mm/s (Figure 3)) but, as seen before, it begins to play an active role when the temperature reaches the value of 200°C.

According to uniaxial tensile test results at different temperatures and strain rates, an initial set of parameters was chosen for each forming condition. The final set of optimized parameters for the whole forming conditions was obtained by using a gradient based optimization algorithm by minimizing the gap between the experimental flow stresses and the predicted flow stresses. Based on the optimization procedure, the final optimized parameters were determined together according to the whole experimental flow stresses curves as shown in Table 1 to Table 3.

The comparisons between experimental data and predicted flow stresses with the three models are shown in Figure 1 to Figure 3. All the three identified hardening laws give a reasonable flow stress description for all the testing conditions within the measured strain range (below~18% for uniaxial tensile tests). However they exhibit very different extrapolations for high strain levels which are frequently encountered in FLDs. For Ludwick's hardening model, the predicted flow stresses all exhibit a monotonic increasing character while the Voce's and H-V models both show a saturation stress state at high strain levels, especially at high temperature and low tensile speed. Because the parameters are generally identified from uniaxial tensile tests, a clear uncertainty exists when hardening modeling is required for the prediction of FLCs at high strain levels. This point will be discussed in the following section.

3 M-K predictive model

3.1 FE M-K model

The classical M-K model assumes an infinite sheet with a planar macroscopic imperfection region where heterogeneous plastic flow develops and localizes. Plastic flow localization is accelerated by nucleation, growth and coalescence of microcavities at the microstructure scale and these phenomena are then considered by introducing a macro-planar defect with maximum porosity

[21]. Due to the difficulties for the mathematical implementation of constitutive models, the implemented yield functions and hardening laws are generally simplistic in classical approaches and not always representative of the actual behaviour of the studied material. Based on the analytical M-K theory, a FE model of the geometrical model was proposed by Zhang et al. [22] to determine numerical FLCs. Due to the symmetry, only half of the entire model is presented. The model is meshed with hexahedral elements. The elasticity behaviour of the material is defined with a Young's modulus of 64000MPa and a Poisson's ratio of 0.3. For the material properties, the three identified hardening behaviours are tested for different strain rates which correspond to the measured strain rates of the Marciniak setup, results are discussed in the next section. Isotropic and anisotropic (Hill48) yield criteria are introduced, the influence of the criterion is also discussed hereafter. For the following results, the isotropic Mises criterion is used. As shown in Figure 4, the initial imperfection value is defined by two different thicknesses in zone a (t_a) and zone b (t_b). In this study, t_b is set to 1 mm, different initial imperfection values of $f_0 = t_b / t_a$ can be obtained by changing the value of t_b .

Due to the initial thickness imperfection, different equivalent plastic strain evolutions are measured in zone a and zone b . When the equivalent plastic strain increment in imperfection region is 7 times greater than in homogeneous zone ($\Delta \bar{\epsilon}_p^B / \Delta \bar{\epsilon}_p^A \geq 7$), localized necking is assumed to occur and the corresponding principal strains of element A ($\bar{\epsilon}_{22}^A, \bar{\epsilon}_{11}^A$) at that moment constitute one limit point of the FLC. To cover the whole FLD, the limit strains with different strain paths can be obtained by imposing different displacement ratios in the in-plane directions. By means of ABAQUS user-defined subroutines, advanced hardening laws and yield functions can be implemented into the FE M-K model for a precise description of the material behaviour.

3.2 Influential parameters

Many research works about the theoretical M-K analysis show that the predicted forming limit strains depend on several factors, such as the imperfection orientation ψ_0 (Figure 4), the imperfection value f_0 and the constitutive model of the sheet material. The critical angle ψ_0 must be chosen for determining the minimum limit strains for the negative strain path in the left hand side of the FLD. The effect of imperfection value and constitutive model will be widely discussed in the last section of this work.

4 Results and discussion

To compare and validate the predicted FLCs, reliable experimental results are essential. The experimental FLCs for AA5086 at different temperatures (20, 150 and 200°C) and equivalent strain rates (0.02, 0.2 and 2s⁻¹) have been determined from a Marciniak device set up on a servo-hydraulic machine. The punch diameter is 40mm and the die radius is 5mm. The pictures at different times were captured with a high speed camera and the strains at the specimen surface were calculated from the DIC technique. By this method, the strain rate is not directly controlled by the machine, it was impossible to have a real-time feedback of the strain measure. The punch speed is controlled during the test and strain rate in the sample is measured after the test. The tested equivalent strain rates (0.02, 0.2 and 2s⁻¹) are calculated by performing an average on the time period between the middle and the end of the test. The details of the specimens, the heating equipment and the procedure to carry out the Marciniak tests at elevated temperatures were introduced in details in [6].

4.1 Predicted FLCs with a constant f_0 value

In the literature, the imperfection value f_0 is defined at room temperature and remains constant for all the forming conditions. From the framework of microstructure, Barlat and Richmond [21]

have adopted a value of 0.996 for f_0 . The same value was also used by Abedrabbo et al. [10] for the FLC prediction of AA5182-O between 25 and 260°C. Hence, for a first approach, this very classical value is tested here. With the Ludwick's hardening model (Eq. 1) and the constant value of 0.996 for f_0 , the comparison between experimental and predictive results is shown in Figure 5.

The predicted FLCs show a good tendency for the temperature sensitivity. But the predicted FLCs deviate from experimental results, especially at 20 and 150°C. An overestimation of all the predicted FLC₀ (major strain value under plane strain condition) values is found. Besides, to evaluate the strain rate influence on the FLCs with the FE M-K model, the FLC₀ have been determined by Ludwick's model with different f_0 values at 200°C (Figure 6) for different forming speeds. Whatever imperfection value is, a positive strain rate effect on the FLC₀ at 200°C is found, which is not consistent with the experimental results. Indeed, a negative effect of strain rate on formability is systematically observed for this aluminium alloy [6].

At first sight, it seems to be difficult to find a constant value for the imperfection for all the tested forming conditions. It could be interesting to determine the appropriate imperfection factor value for each condition and for each hardening law to discuss the validity of the M-K model and the influence of thermo-viscoplastic behaviour modeling of AA5086.

4.2 Calibration strategy

The calibration of the geometrical imperfection f_0 has been formulated as an inverse problem and explained with more details in the previous work [6]. The calibration method is based on the specific point in plane strain conditions (FLC₀) which is frequently critical for the forming of industrial parts. Moreover, in the M-K model, this point is not sensitive to the choice of the yield criterion. The evolutions of the predicted FLC₀ values at different temperatures with the f_0

calibrated at the three experimental temperatures, for a strain rate of 2s^{-1} , are shown in Figure 7. The predicted values give a rather good evolution tendency with the forming temperature. The minimum FLC_0 is found between 100 and 150°C which coincides globally with experimental observations made at different forming speeds. Once more, for the Ludwick's law, a calibration is required for each temperature and a constant imperfection value does not permit to reproduce the experimental results.

4.3 Influence of the hardening law

In this section, from the three identified hardening models, the validity of the predicted FLCs determined with f_0 values calibrated under each forming condition is discussed. The first objective is to evaluate the correlation between the whole calibrated FLCs and the experimental ones, and the second is to verify if a calibration is really necessary for each forming condition, irrespective of hardening law.

4.3.1 FLCs predicted with the Ludwick's hardening model

The calibrated f_0 values with Ludwick's hardening model under each forming condition are shown in Table 4. Clearly, the calibrated f_0 values vary with temperature and strain rate. With these calibrated values, the predicted FLCs at different temperatures and strain rates are shown in Figure 8 to Figure 10. Good formability predictions are observed over the tested temperature and strain rate ranges, especially for the left hand side of the Forming Limit Diagram. The results prove that the FE M-K model could be an efficient tool to predict the FLCs under different temperatures and strain rates on condition that the initial imperfection is calibrated for each forming condition but with only one point (FLC_0).

4.3.2 FLCs predicted with the Voce's hardening model

The calibrated f_0 values with Voce's hardening model under each forming condition are shown in Table 5. Unfortunately, it cannot give reasonable predictions of FLCs for high temperatures and low forming speeds, even though the initial imperfection is almost set to 1. The predicted FLCs are presented in Figure 11.

For a strain rate of $2s^{-1}$, the Voce's hardening model gives a good prediction of FLCs over the tested temperature range. Compared with the FLCs predicted by Ludwick's model for the same magnitude of strain rate (Figure 12), the Voce's model gives a better prediction for the right hand side of the FLD. The trend of the Ludwick's law is to underestimate the experimental results while the Voce's law leads to an overestimation of these results. This difference can be explained by the two different characters of the hardening laws but also by the choice of the yield function. Indeed, the yield function affects only the right hand side of the FLD. To illustrate this purpose, the comparison of the predicted FLCs from Ludwick's and Voce's hardening models associated with two yield functions are shown in Figure 13, at $20^{\circ}C$ and $2s^{-1}$. The anisotropy of this alloy is relatively low in the plane of the sheet and does not present abnormal behaviour (for AA5086, its biaxial yield stress is larger than uniaxial yield stress), so Hill48 yield criterion can give an acceptable description of this anisotropy even if a criterion with two linear transformation tensors (Bron and Besson) was shown to be better for this material [23]. Temperature effect is included in the yield stress definition (Eq. 4) but we suppose that the shape of the yield function is not affected by temperature, which is confirmed by the 2D-plots with normalized stresses for different temperatures in [8]. It is found that for the right hand side of the FLCs, the Ludwick's hardening model associated with Hill48 (Table 6) yield function gives a very good prediction, while for

Voce's hardening model, the isotropic von Mises yield function gives the best predictions. For the right hand side of the FLCs, the choice of the yield function remains strongly coupled with the choice of the hardening model. Depending on the hardening model, the use of the anisotropic Hill48 criterion on forming limits, can improve or degrade the numerical predictions. A complex and more adapted yield function will give better results only if a precise hardening model is adopted. The effects of yield function are the same for the other forming conditions, not presented here.

4.3.3 FLCs predicted with the H-V hardening model

The calibrated f_0 values with H-V hardening model under each forming condition are shown in Table 7. The predicted FLCs at $2s^{-1}$ are presented in Figure 14. A rather good correlation is observed at 20°C, while for high temperatures, the predicted FLCs show an overestimation in the right hand side, especially for equibiaxial strain paths. Similarly to the Voce's hardening model, the mixed H-V model is not able to predict AA5086 formability at high temperatures and low forming speeds.

As mentioned above, uncertainties exist for the identified parameters based on the uniaxial tensile test data, especially at high strain levels. These uncertainties are responsible for an overestimation of the saturation effect of the Voce and H-V models at high temperatures and low forming speeds (Figure 1). With an overestimated saturation, premature necking will develop, which explains that the imperfection must be very small to delay the onset of necking. For these specific conditions, whatever the size of the imperfection is, it was impossible to correlate the predicted and experimental forming limits by adjusting the imperfection value. The different strain hardening characters and the parameter uncertainty of the proposed models lead to very different calibrated imperfection values of the M-K model under the same forming conditions. Uniaxial

tensile tests are inappropriate to characterize the material hardening behaviour for forming applications. The identification of hardening parameters must be completed from experimental data achieved at high strain levels. Bulge tests or biaxial tensile tests with cruciform specimens are more appropriate since the measured equivalent strain level can be two times larger than the one in uniaxial tensile test.

5. Conclusion

Hardening behaviour of metallic sheets is usually identified from uniaxial tensile tests. The main purpose of this work was to evaluate the uncertainty on the forming limit predictions when the classical uniaxial tensile test is used to evaluate the thermo-viscoplastic behaviour of an aluminium alloy for different forming conditions. Then, based on uniaxial tensile test results at different temperatures and strain rates, three very different hardening models have been proposed to correlate the experimental curves. All the three hardening models give a good flow stress correlation for the whole temperature and strain rate ranges, for an equivalent strain level below 20%. Due to the low homogeneous strain level reached in uniaxial tensile test, great differences of flow stress extrapolation appear at high strain levels between the three models.

With the identified hardening models, predicted FLCs are determined from the FE M-K model and are compared to experimental FLCs. For a given hardening law, the calibrated imperfection values f_0 of the M-K model vary with the forming conditions which limits significantly the use of the predictive M-K model without any experimental data. Nevertheless, only one test in a plane strain state for each condition is sufficient to calibrate precisely the model and to give an accurate estimation of the whole FLC. For given forming conditions, the imperfection value depends on the choice of the hardening law: for example, at ambient temperature and for a strain rate of 2s^{-1} ,

$f_0=0.95$ for Ludwick's model, 0.99 for Voce model and 0.975 for H-V model. For some conditions (high temperatures and low forming speeds), the saturation effect of Voce and H-V models is overestimated which leads to premature necking and strong difficulties in adjusting the imperfection value of the M-K model. As shown, the choice of the yield function remains strongly coupled with the choice of the hardening model. As an example, the use of the anisotropic Hill48 criterion, instead of the isotropic Mises criterion, can improve (Ludwick's model) or degrade (Voce's model) the predicted forming limits.

In order to remove the strong uncertainty on the choice of the hardening model, tests at high strain levels are required. This can be achieved with bulge tests or biaxial tensile tests with cruciform specimens. A work is in progress and will be published soon with the last device, for the same material. The results presented on the two extreme laws (Ludwick and Voce) show that it would be difficult to keep a constant value f_0 for all the forming conditions. Maybe, this can be explained by the definition of the macro-imperfection of the M-K model which is directly linked to the behaviour of the microstructure. Complex phenomena at the microstructure scale are certainly affected by the forming temperature or strain rate and a solution should consist in expressing the imperfection factor with temperature and strain rate in order to make reliable the model on a wide range of forming conditions with limited calibration steps.

Acknowledgements

The authors would like to acknowledge financial support from National Natural Science Foundation of China (Grant No. 51405266) and Natural Science Foundation of Shandong Province (Grant No. ZR2014EEP003).

References

1. T. Naka, G. Torikai, R. Hino, and F. Yoshida, The effects of temperature and forming speed on the forming limit diagram for type 5083 aluminum-magnesium alloy sheet, *J. Mater. Process. Technol.*, 2001, 113(1-3), p 648 - 653.
2. D. Li and A. K. Ghosh, Tensile deformation behavior of aluminum alloys at warm forming temperatures, *Mater. Sci. Eng., A*, 2003, 352(1), p 279 - 286.
3. D. Li and A. K. Ghosh, Biaxial warm forming behavior of aluminum sheet alloys, *J. Mater. Process. Technol.*, 2004, 145(3), p 281 - 293.
4. G. Palumbo and L. Tricarico, Numerical and experimental investigations on the warm deep drawing process of circular aluminum alloy specimens, *J. Mater. Process. Technol.*, 2007, 184(1-3), p 115 - 123.
5. W. Hui, Y. B. Luo, P. Friedman, M. H. Chen and G. A. O. Lin, Warm forming behavior of high strength aluminum alloy AA7075, *Trans. Nonferrous Met. Soc. China*, 2012, 22(1), p 1 - 7.
6. X. Chu, L. Leotoing, D. Guines, and E. Ragneau, Temperature and strain rate influence on AA5086 forming limit curves: Experimental results and discussion on the validity of the M-K model, *Int. J. Mech. Sci.*, 2014, 78, p 27-34.
7. A. S. Khan and M. Baig, Anisotropic responses, constitutive modeling and the effects of strain-rate and temperature on the formability of an aluminum alloy, *Int. J. Plast.*, 2011, 27, p 522 - 538.
8. N. Abedrabbo, F. Pourboghrat, and J. Carsley, Forming of aluminum alloys at elevated temperatures - Part 1: Material characterization, *Int. J. Plast.*, 2006, 22, p 314 - 341.
9. N. Abedrabbo, F. Pourboghrat, and J. Carsley, Forming of aluminum alloys at elevated temperatures - Part 2: Numerical modeling and experimental verification, *Int. J. Plast.*, 2006, 22, p 342 - 373.
10. N. Abedrabbo, F. Pourboghrat, and J. Carsley, Forming of AA5182-O and AA5754-O at elevated temperatures using coupled thermo-mechanical finite element models, *Int. J. Plast.*, 2007, 23(5), p 841 - 875.
11. F.J. Zerilli and R.W. Armstrong, Dislocation-mechanics-based constitutive relations for material dynamics calculation, *J. Appl. Phys.*, 1987, 5, p 1816 - 1825.
12. Y. Bergstrom, Dislocation model for the stress-strain behaviour of polycrystalline alpha-iron with special emphasis on the variation of the densities of mobile and immobile dislocations, *Mater. Sci. Eng.*, 1969, 5, p 193 - 200.
13. S. Nemat-Nasser and Y. Li, Flow stress of fcc polycrystals with application to OFHC cu, *Acta Mater.*, 1998, 46(2), p 565 - 577.
14. G. Z. Voyiadjis and F. H. Abed, Microstructural based models for bcc and fcc metals with temperature and strain rate dependency, *Mech. Mater.*, 2005, 37(2-3), p 355 - 378.
15. A. Rusinek and J. R. Klepaczko, Shear testing of a sheet steel at wide range of strain rates and a constitutive relation with strain-rate and temperature dependence of the flow stress, *Int. J. Plast.*, 2001, 17(1), p 87 - 115.
16. A.H. van den Boogaard and P.J. Bolt, A material model for warm forming of aluminium sheet, In VII International conference on computational plasticity, COMPLAS, 2003.
17. H. Vegter, C. Horn, Y. An, E. H. Atzema, H. Pijlman, T. H. van den Boogaard, and H. Huetink, Characterization and modelling of the plastic material behaviour and its application in sheet metal forming simulation, VII International Conference on Computational Plasticity, Barcelona, 2003.
18. A. Rusinek and J.A. Rodríguez-Martínez, Thermo-viscoplastic constitutive relation for aluminium alloys, modeling of negative strain rate sensitivity and viscous drag effects, *Mater. Des.*, 2009, 30(10), p 4377 - 4390.
19. H. Aretz, An extension of Hill's localized necking model, *Int. J. Eng. Sci.*, 2010, 48, p 312 - 331.
20. J. H. Sung, J. H. Kim, and R.H. Wagoner, A plastic constitutive equation incorporating strain, strain-rate, and temperature, *Int. J. Plast.*, 2010, 26(12), p 1746 - 1771.
21. F. Barlat and O. Richmond, Modelling macroscopic imperfections for the prediction of flow localization and fracture, *Fatigue Fract. Eng. Mater. Struct.*, 2003, 26, p 311 - 321.

22. C. Zhang, L. Leotoing, G. Zhao, D. Guines, and E. Ragneau, A methodology for evaluating sheet formability combining the tensile test with the M-K model, *Mater. Sci. Eng., A*, 2010, 528(1) , p 480 - 485.
23. S. Zhang, L. Leotoing, D. Guines, S. Thuillier, and S. Zang, Calibration of anisotropic yield criterion with conventional tests or biaxial test, *Int. J. Mech. Sci.*, 2014, 85, p 142-151.

Table captions

Table 1

Optimized parameters of the proposed Ludwick's model

Table 2

Optimized parameters of the proposed Voce's model

Table 3

Optimized parameters of the proposed H-V model

Table 4

Calibrated f_0 values for the different forming conditions by Ludwick's hardening model

Table 5

Calibrated f_0 values for the different forming conditions by Voce's hardening model

Table 6

Parameter values of Hill48 yield function for AA5086

Table 7

Calibrated f_0 values for the different forming conditions by H-V hardening model

Table 1: Optimized parameters of the proposed Ludwick's model

$K_0 (MPa)$	$K_1 (MPa/^\circ C)$	n_0	$n_1 (1/^\circ C)$	m_0	$m_1 (1/^\circ C)$
537.41	0.975	0.567	0.00072	0.000088	0.0319

Table 2: Optimized parameters of the proposed Voce's model

$K_3 (MPa)$	$K_4 (1/^\circ C)$	K_5	$K_6 (1/^\circ C)$	m_2	$m_3 (1/^\circ C)$
485.96	0.00453	0.943	0.009	0.000092	0.0315

Table 3: Optimized parameters of the proposed H-V model

α_1	$\alpha_2 (1/^\circ C)$	$K_7 (MPa)$	n_2
0.683	0.00253	633.11	0.613
$K_8 (MPa)$	K_9	m_4	$m_5 (1/^\circ C)$
136.82	28.14	0.000093	0.0319

Table 4: Calibrated f_0 values for the different forming conditions by Ludwick's hardening model

Temperature (°C)	Strain rate (1/s)	Calibrated f_0
20	2	0.9507
150	2	0.97
200	2	0.9927
150	0.2	0.99
200	0.2	0.99985
150	0.02	0.99985

Table 5: Calibrated f_0 values for the different forming conditions by Voce's hardening model

Temperature (°C)	Strain rate (1/s)	Calibrated f_0
20	2	0.9908
150	2	0.997
200	2	0.99999

Table 6: Lankford's coefficients and Hill48 yield parameters for AA5086

r_0	r_{45}	r_{90}	F	G	H	L	M	N
0.57	0.52	0.62	0.7	0.636	0.363	1.5	1.5	1.494

Table 7: Calibrated f_0 values for the different forming conditions by H-V hardening model

Temperature (°C)	Strain rate (1/s)	Calibrated f_0
20	2	0.975
150	2	0.999
200	2	0.99995

Figure captions

Figure 1: Flow stresses predicted by different hardening models with equivalent strain up to 50% and comparison with experimental data at 1 mm/s.

Figure 2: Flow stresses predicted by different hardening models with equivalent strain up to 50% and comparison with experimental data at 10 mm/s.

Figure 3: Flow stresses predicted by different hardening models with equivalent strain up to 50% and comparison with experimental data at 100 mm/s.

Figure 4: FE M-K model.

Figure 5: Predicted FLCs by Ludwick's model with constant $f_0=0.996$ and a strain rate of $2s^{-1}$.

Figure 6: FLC₀ with different values of f_0 by Ludwick's model at 200°C.

Figure 7: Evolution of FLC₀ with Ludwick's model and for a calibration at different temperatures (strain rate of $2s^{-1}$).

Figure 8: Predicted FLCs at 20°C with Ludwick's model.

Figure 9: Predicted FLCs at 150°C with Ludwick's model.

Figure 10: Predicted FLCs at 200°C with Ludwick's model.

Figure 11: Predicted FLCs by Voce's model at different temperatures and for a strain rate of $2s^{-1}$.

Figure 12: Predicted FLCs by Ludwick's model at different temperatures and for a strain rate of $2s^{-1}$.

Figure 13: FLCs predicted from Ludwick's and Voce's models with different yield functions at 20°C and $2s^{-1}$.

Figure 14: Predicted FLCs by H-V model at different temperatures and for a strain rate of $2s^{-1}$.

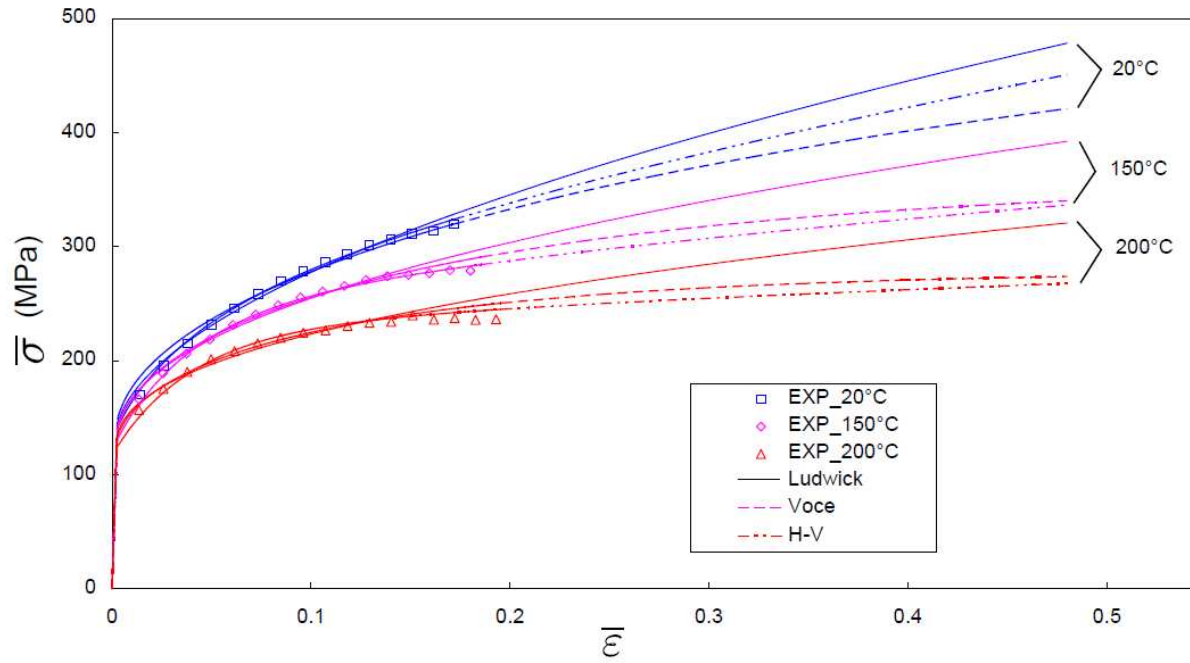


Figure 1: Flow stresses predicted by different hardening models with equivalent strain up to 50% and comparison with experimental data at 1 mm/s.

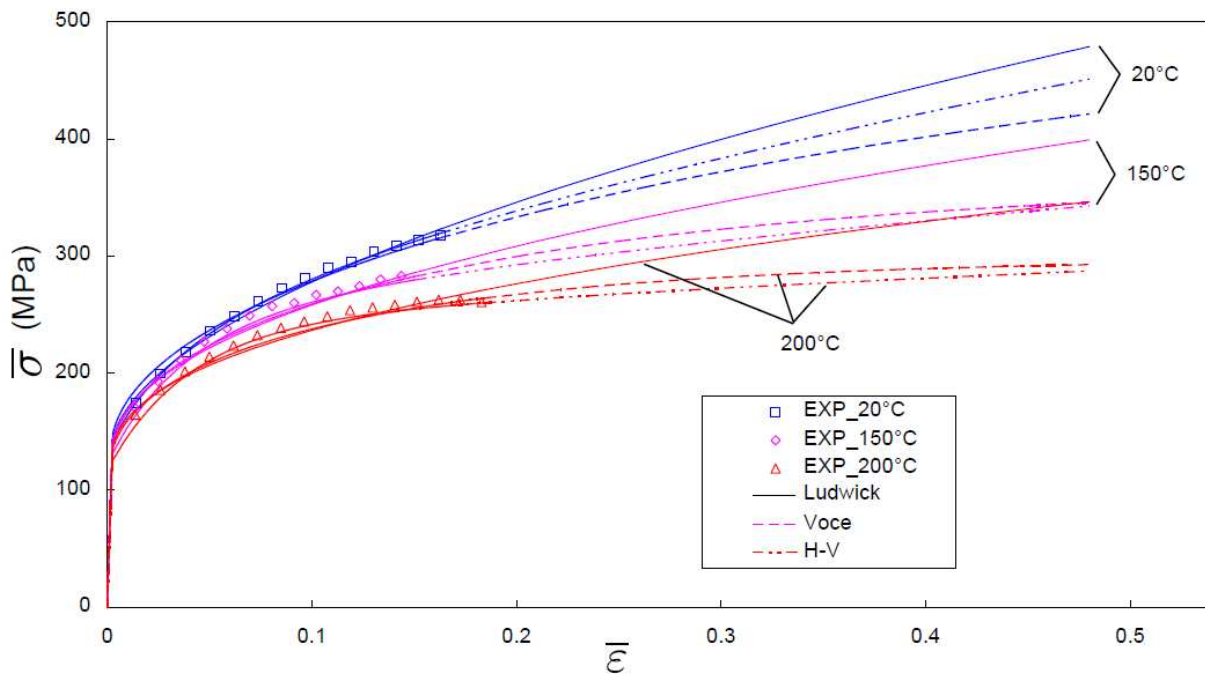


Figure 2: Flow stresses predicted by different hardening models with equivalent strain up to 50% and comparison with experimental data at 10 mm/s.

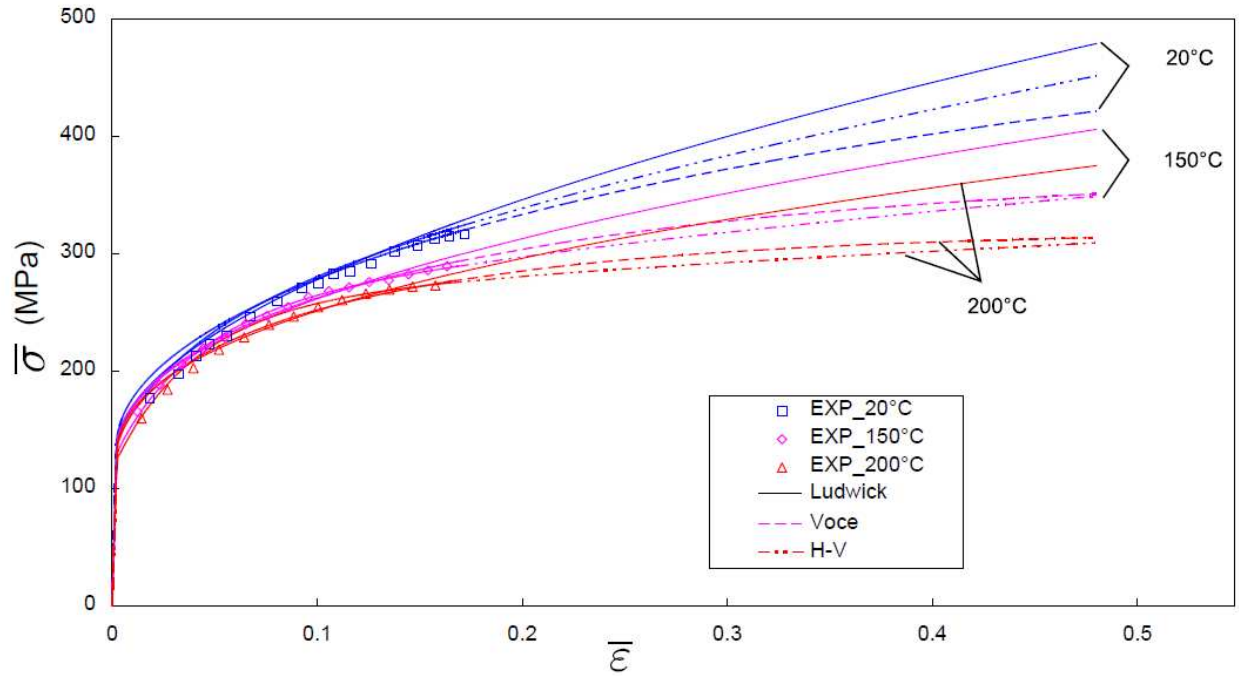


Figure 3: Flow stresses predicted by different hardening models with equivalent strain up to 50% and comparison with experimental data at 100 mm/s.

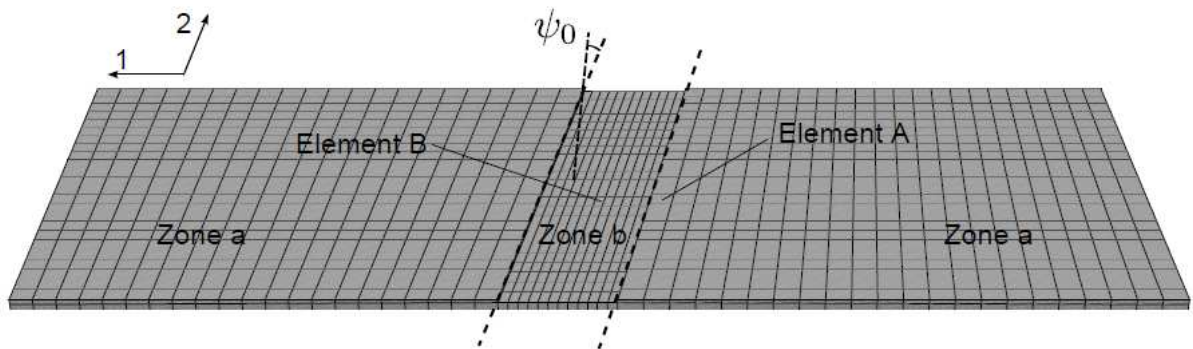


Figure 4: FE M-K model.

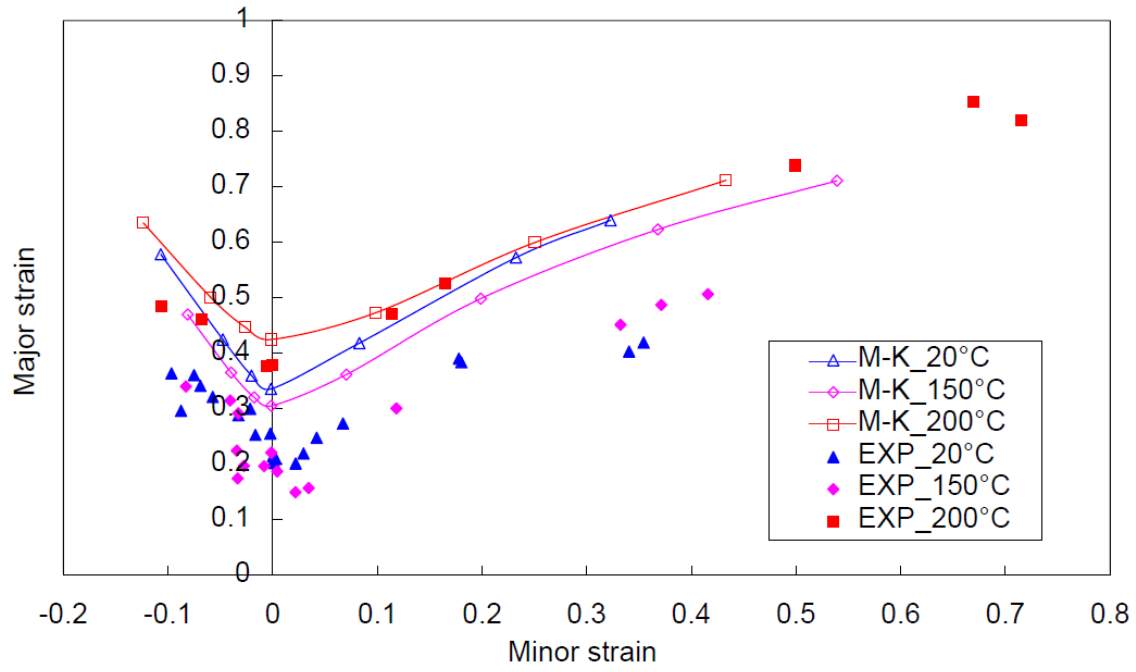


Figure 5: Predicted FLCs by Ludwick's model with constant $f_0=0.996$ and a strain rate of $2s^{-1}$.

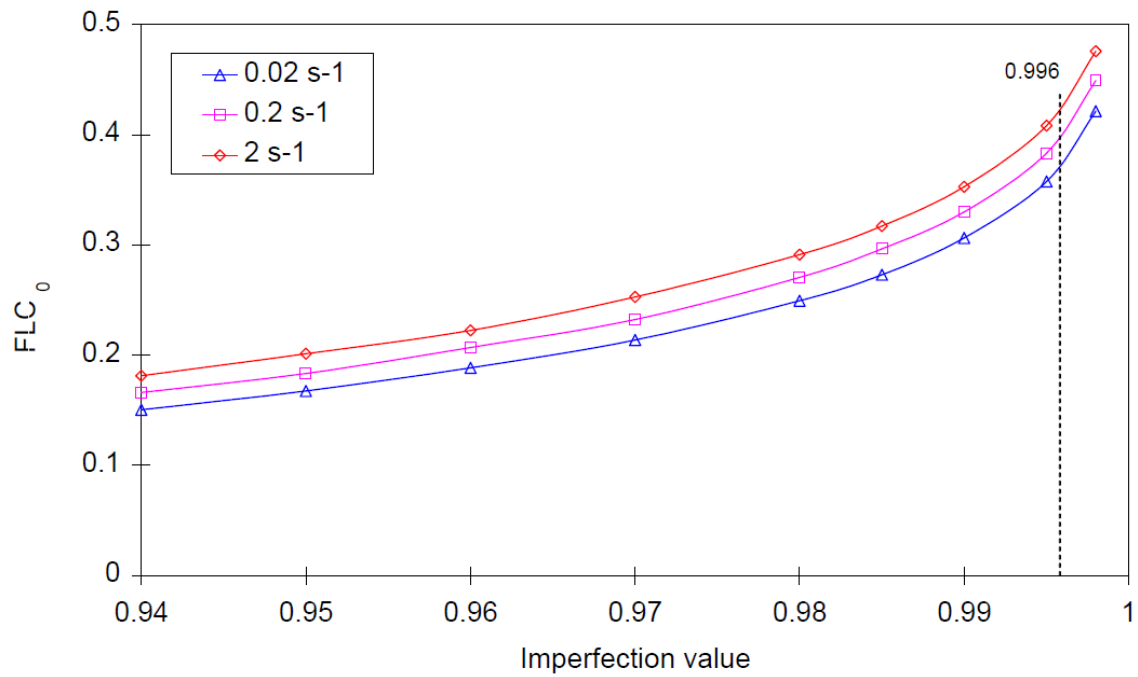


Figure 6: FLC_0 with different values of f_0 by Ludwick's model at $200^\circ C$.

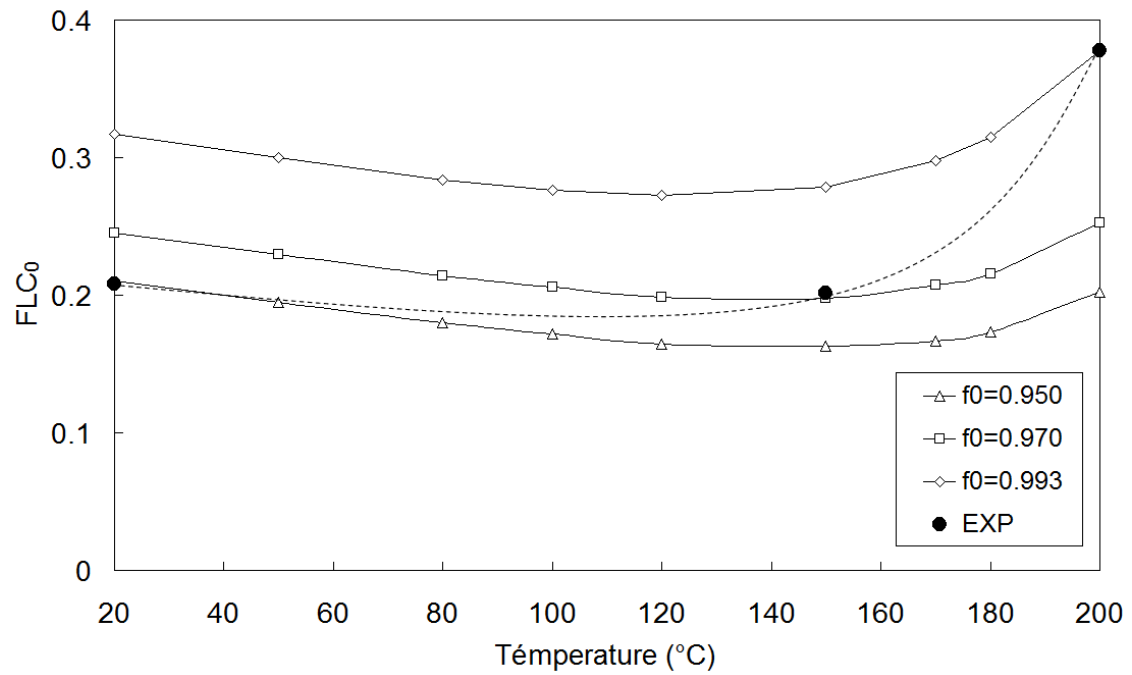


Figure 7: Evolution of FLC_0 with Ludwick's model and for a calibration at different temperatures (strain rate of $2s^{-1}$).

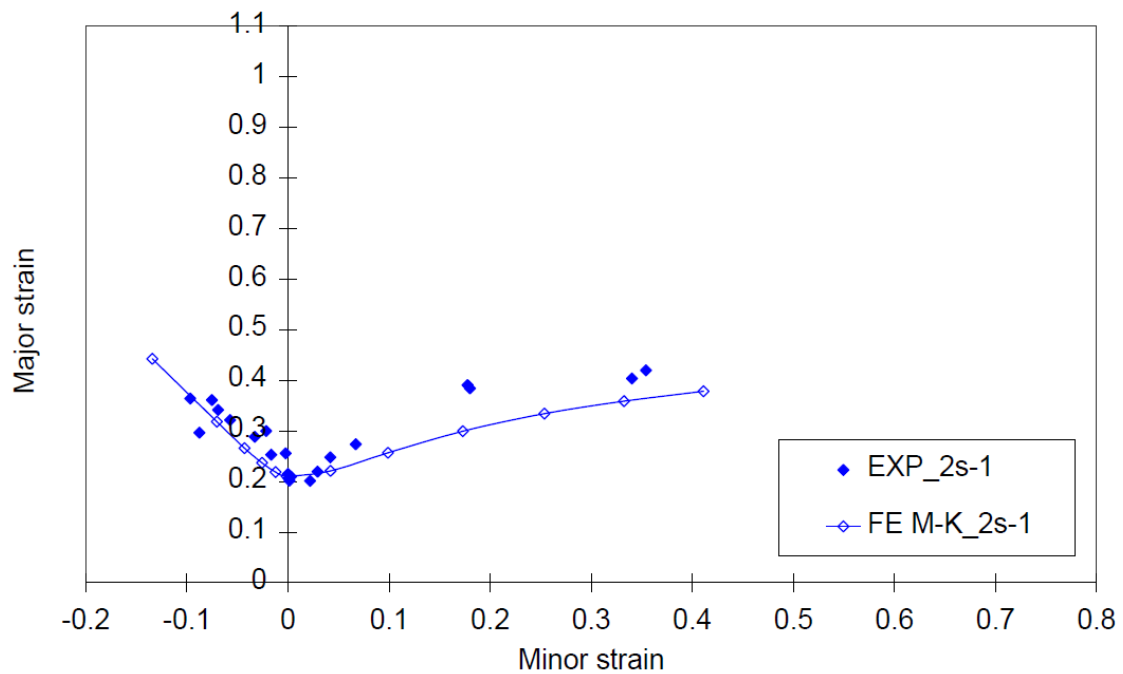


Figure 8: Predicted FLCs at 20°C with Ludwick's model.

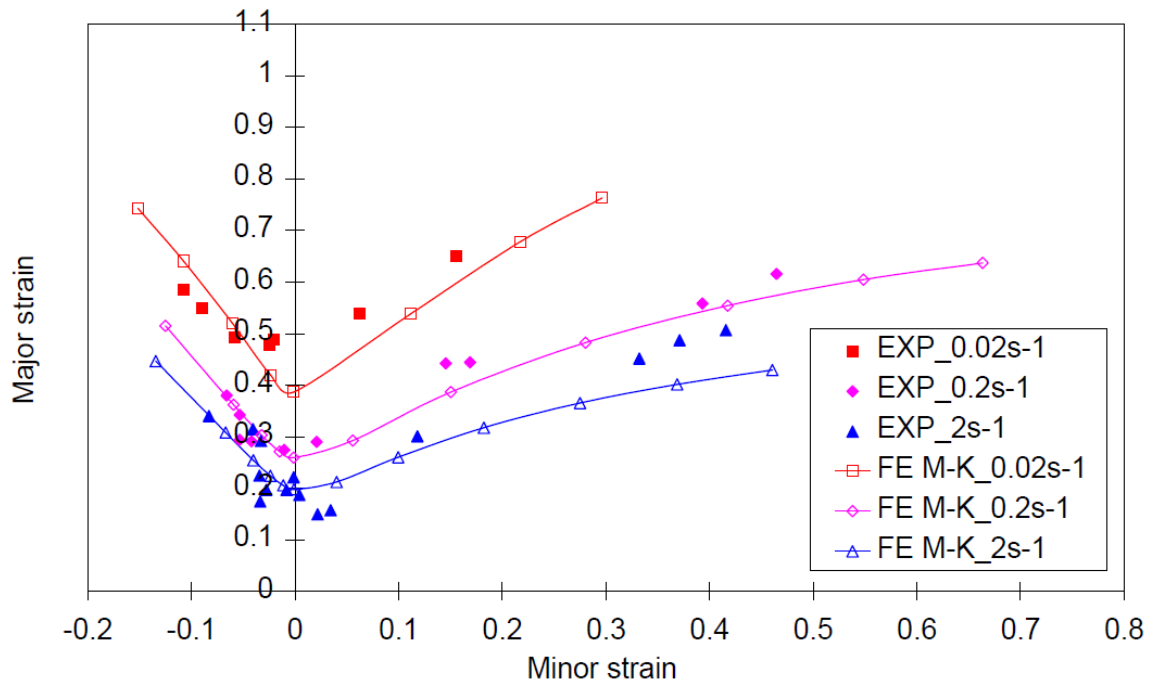


Figure 9: Predicted FLCs at 150°C with Ludwick's model.

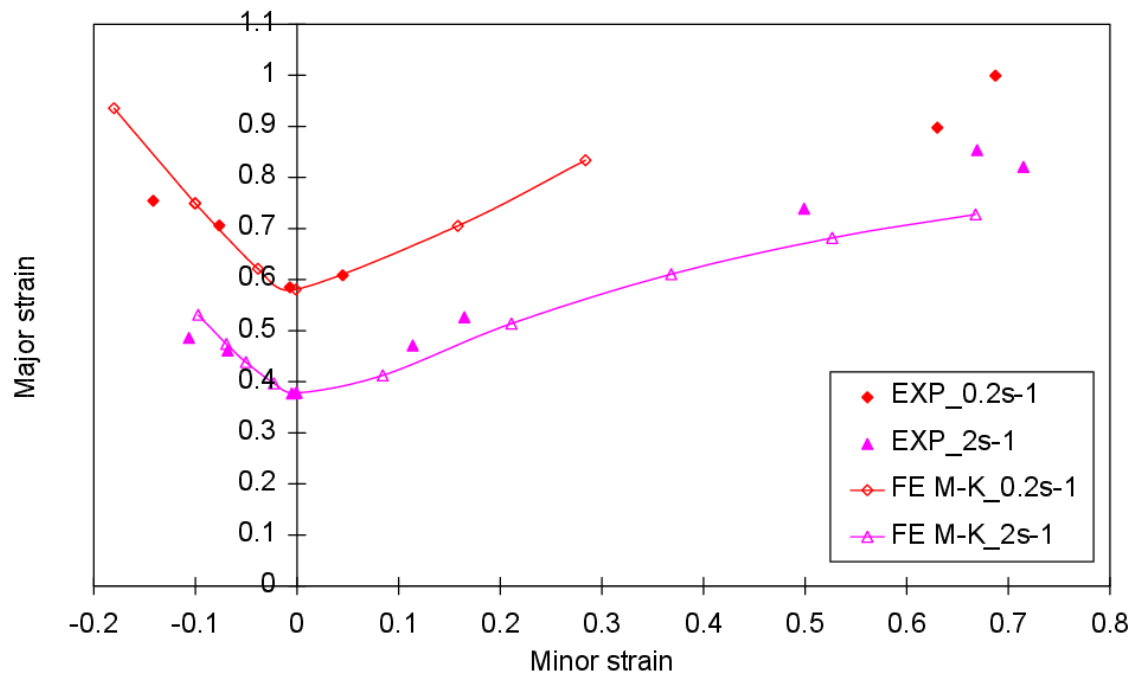


Figure 10: Predicted FLCs at 200°C with Ludwick's model.

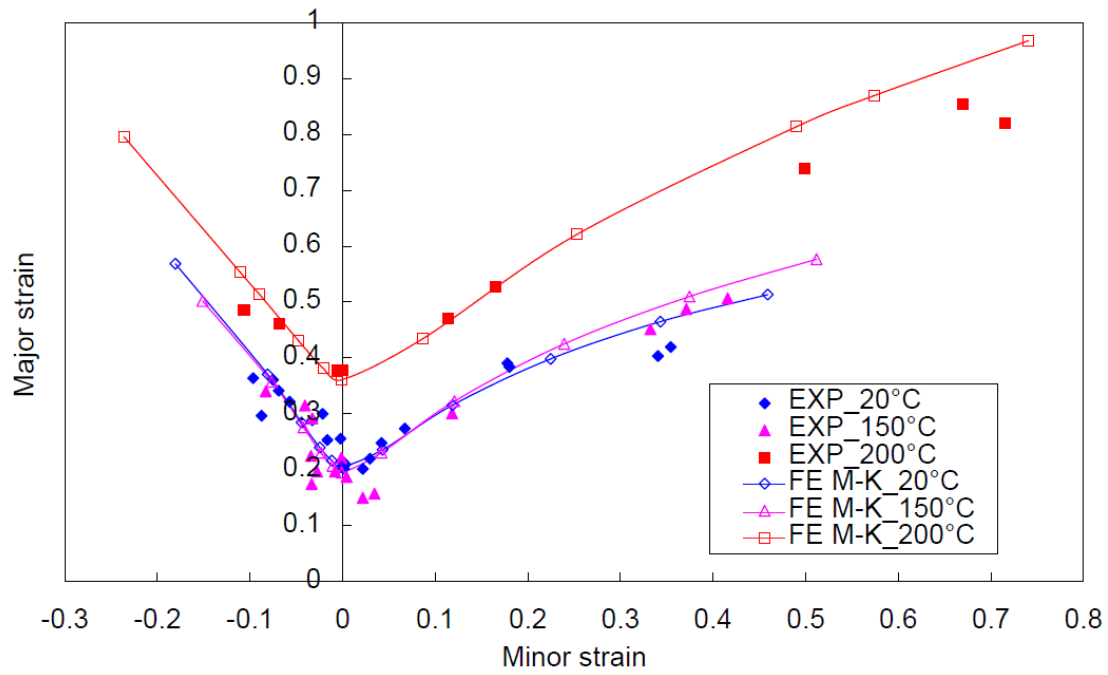


Figure 11: Predicted FLCs by Voce's model at different temperatures and for a strain rate of $2s^{-1}$.

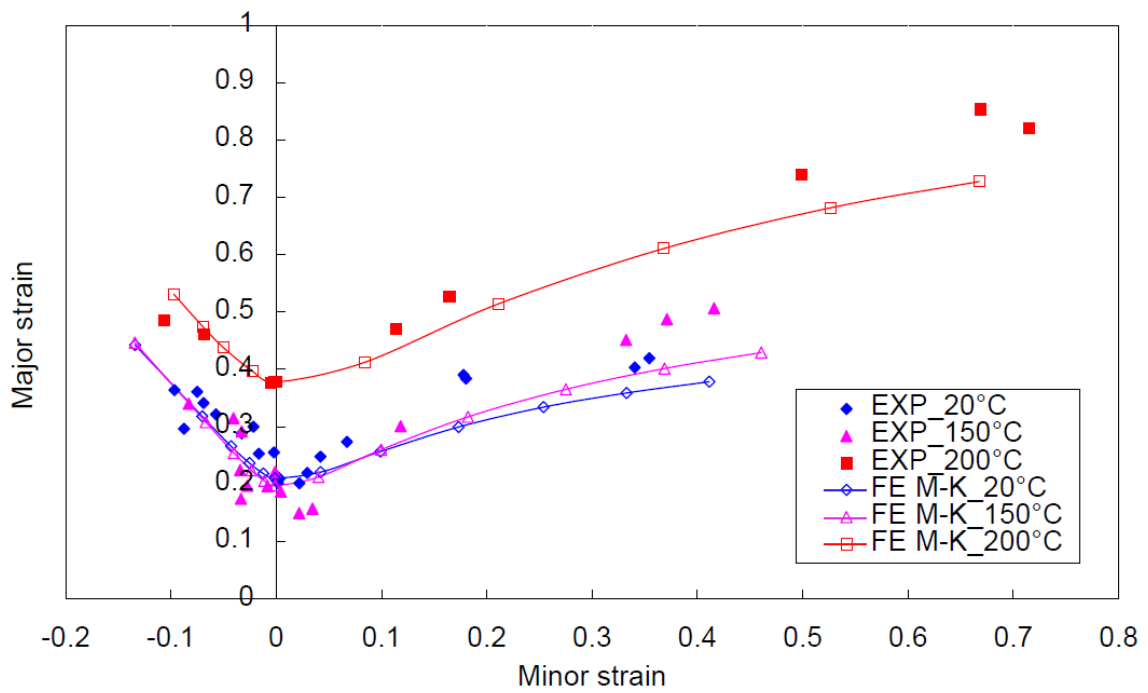


Figure 12: Predicted FLCs by Ludwick's model at different temperatures and for a strain rate of $2s^{-1}$.

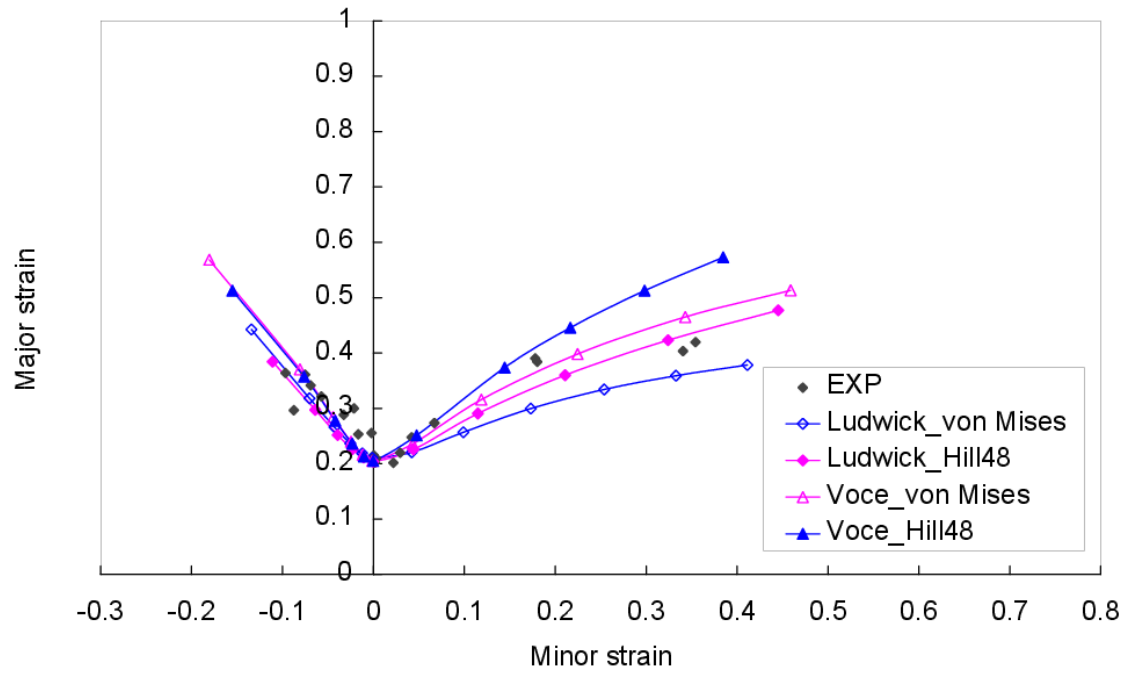


Figure 13: FLCs predicted from Ludwick's and Voce's models with different yield functions at 20°C and $2s^{-1}$.

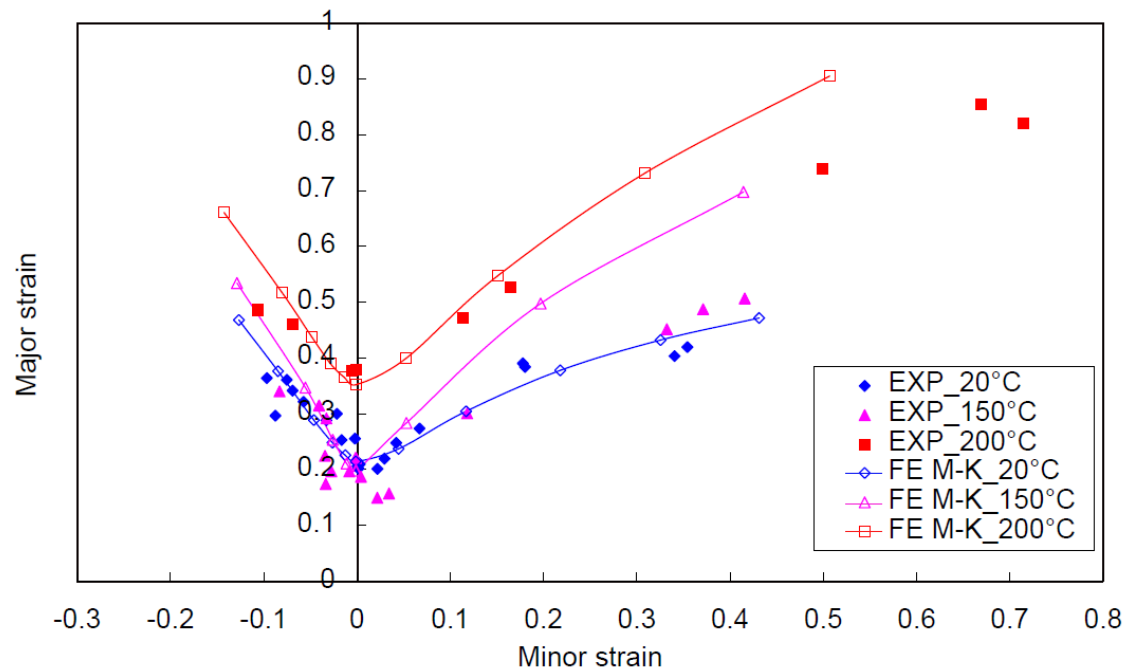


Figure 14: Predicted FLCs by H-V model at different temperatures and for a strain rate of $2s^{-1}$.